Turk J Phys
27 (2003) , 51 – 59.

Multiply Charged Ions Produced after Deexcitation Processes for Important Elements in Astrophysics

Adel M. EL-SHEMI, Adel A. GHONEIM
College of Technological Studies, Department of Applied Sciences,
P.O. Box 42325 Shuwaikh, 70654 KUWAIT
Yehia A. LOTFY
El-Minia University, Faculty of Science, Physics Department,
61111 El-Minia-EGYPT

Received 10.10.2000

Abstract

Selection random number method (Monte Carlo technique) is used to calculate the ion charge state distributions (CSD) and mean ion charge $\bar{q}$ after K-, L_I, L_{III}- and M_I- shell ionization in neutral atoms and their q-fold ground state ions (q = 0 to 10) from C to Fe elements. Atomic data for radiative and non-radiative transitions and electron shake off process, which is used in the modeling vacancy cascade program, are computed with relativistic wave functions. Use of atomic data is important to accurately model vacancy cascades. To enhance the agreement between calculated and experimental values, the electron shake-off processes and shifts of the electron energy level during vacancy cascade propagation have been considered. The results obtained from present calculations reasonably agree with other calculation and experimental spectra.

Key Words: Auger Cascade, Ion charge state distributions, Monte Carlo technique

1. Introduction

The ionization of an inner-shell electrons leaves the atomic system in a very unstable electronic configuration which may decay by either a radiative or non- radiative transitions. The filling of an inner-shell vacancy in an atom or ion may produce new vacancies in higher shells which can then be filled by further radiative and/or non-radiative transitions. Such successive transitions during the atomic reorganization, known as a vacancy cascade process, continues until all vacancies reach the outermost occupied shell. Thus very high charge states are ultimately produced. During the vacancy-cascade development many photons and Auger electrons may be emitted. In addition to the vacancy filling processes (x-ray and Auger transitions), there is an electron shake-off process. It can be interpreted as when a vacancy is created, there is a small probability that an electron in another shell will be excited to an unoccupied bound state or ejected into the continuum as the result of the sudden change of atomic potential. This secondary process causes additional vacancies during the vacancy cascade development and plays an important role in the final charge state distribution (CSD) of ions.

Extensive experimental and theoretical studies of vacancy cascades after inner shell vacancy production have been reported in a number of works. Snell [1] measured the charge state ions for rare gases after nuclear decay using a charge spectrometer.

Carlson and Krause [2], Carlson et al. [3], and Krause and Carlson [4] have measured CSD produced by inner-shell photoionization in rare gas atoms using photons energies obtained from x-ray tubes. Hastings et al. [5], Tonuma et al. [6], Hayashi et al. [7] and Mukoyama et al. [8] have investigated the vacancy cascade

for Kr and Xe as a function of photon energy using synchrotron radiation (SR) and time of flight (TOF) spectrometer. Atomic rearrangement of fast heavy ions passing through solid targets has been studied using simulation method by Mukoyama [9].

Understanding of CSD can be applied to calculating the ionization equilibrium of interstellar gas, involving CSD atomic data for various atoms and ions. In particular, such data are collected for elements up to Ar [10] and is important for studying the production and storage of cold ions [11]. Charge multiplying cascades are also of interest for understanding basic processes in electron impact ion sources [12]. The knowledge of the ion charge state distribution (CSD) is necessary to study plasma diagnostic [13].

In the calculation of vacancy cascades, techniques that either use only the most important radiative and non-radiative transitions involved in filling the various vacancies in atoms [14], or random selection techniques i.e. Monte-Carlo techniques have been considered. Carlson and Krause [15] and Mukoyama [16] have estimated the charge distribution of ions following inner-shell vacancy production for Ar, Kr and Xe. They traced successive x-ray and Auger transitions via a Monte Carlo technique. Mirakhmedov and Parilis [17] discussed a calculation of a vacancy cascade for Kr. They took to consideration during cascade development some Auger channels that turn out to be energetically forbidden due change in the electron binding energy.

Opendak [18] used a Monte Carlo method to simulate vacancy cascade following inner-shell vacancy production in atoms and their ground state ions of Z = 11 to 26. The data for radiative and non-radiative transition for single ionized atoms, used in their computer model, were collected from various literature sources [19,20,21,22]. The electron shake off, which results from a sudden change in atomic potential and Auger channels that turn out to be energetically forbidden due to the change in the electron binding energy are neglected in his calculations.

In the present paper, we present results of our study of CSD of ions and the probabilities p(q) associated with various inner-shell vacancies in ionized atoms and their q-fold ground state ions ($0 \leq q \leq 10$) from C up to Fe. A Monte Carlo method is used to simulate the vacancy cascade. In the study of CSD for ions, the problem is that, for most elements, consistent sets of atomic data are not available. Therefore, radiative transition data for single ionized atoms and their ground state ions are calculated with the Nonortho program developed by Reiche [23] using Multiconfiguration Dirac-Fock (MCDF) wavefunctions performed with the Grasp-code [24,25,26]. The non-radiative transitions using Dirac-Fock-Slater (DFS) wavefunctions were computed with a code written by Lorenz and Hartmann [27]. Electron shake-off probabilities were computed using a computer code written by El-Shemi [28]. The closing of energetically forbidden Auger and Coster-Kronig channels, which occurs due to multiple-vacancy creation in the atomic structure, and the electron shake-off process are considered in our calculation. The present results are compared with both theoretical and experimental values.

2. Theoretical Analysis

A Monte Carlo method has been used to calculate the vacancy cascades produced after inner-shell ionization in atoms and their ground state ions. The calculation is accomplished after consideration of all possible radiative (x-ray), non- radiative (Auger-and Coster-Kronig) transitions and electron shake-off probabilities. Analysis of the cascade are described in details in [29,30]. To realize a Monte Carlo selection of the actual de-excitation channel, the probabilities of all de-excitation channels were normalized to one. The random number generated in the interval (0,1) selects the next de-excitation step, including vacancy transfer and ionization. After production a new vacancy in an actual subshell, the program at first controls whether shake-off takes place or not. If the sum of all normalized shake-off probabilities of the preceding vacancy configuration is greater than the random number, then a shake-off process takes place. The channel whose subshell shake-off probability value coincides with the random number generated will be activated. After the decision about the occurrence of shake-off processes, the program selects the next de-excitation channel by generating a new random number. The value of the random number is compared with the value of fluorescence yield to determine whether radiative or non-radiative transitions take place. Following this decision the actual de-excitation channel is chosen in analogy with the determination of the shake-off channels. For each new vacancy the program code goes back to the first step described above. The generation of new vacancy configurations continues until all vacancies have reached the outer shell (i.e. an

energetically stable state). Then the number of vacancies is recorded. After finishing off a cascade the same initial vacancy will once more be set in the considered inner shell and the cascade will be simulated again. After 10^5 histories the charge state distribution CSD of ions and average ion charge state, q, are recorded.

The creation of multiple vacancies in atomic configurations during vacancy population causes transition energy shifts [31] and may result in an energetic closing of channel for certain Coster-Kronig transitions. In the determination of the population of the multiple vacancy states, the vacancy cascade modeling takes into account the fact that the change of radiative and non-radiative transition rates due to transition energy shifts. The correction of the transition rates quantum mechanically requires more complex calculations. Therefore the transition rates were calculated according to the following scheme. At first, quantum mechanically determined transition rates were calculated for single ionized atoms and ground state ions. Then for all other configuration with more vacancies, the corrected transition rates are calculated using the scaling procedure proposed by Larkins [32]. The comparison between quantum mechanically calculated results and the corresponding results based on scaling procedure method shows that the deviation of the change of transition rates is not significant, as shown in Figure 1 for K-x-ray multiply ionized neon. So, the corrected transition rates during vacancy cascade development are obtained using the scaling procedure.

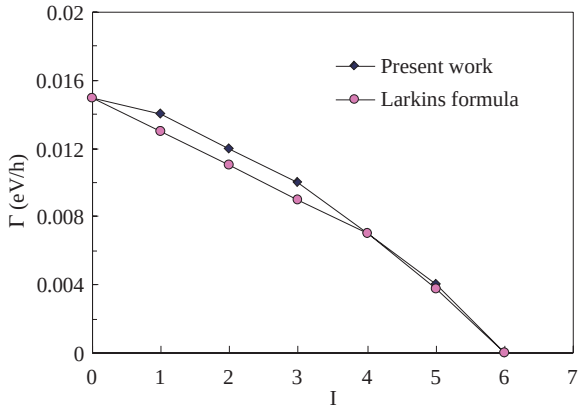

Figure 1. Comparison of K x-ray for multiply ionized neon between our exact Quantum mechanical calculation and statistical method [32].

3. Results and Discussions

During the cascade propagation electron transitions are accompanied by shifts of the electron energy levels, from which some initially allowed Coster-Kronig transition may be become energy forbidden. Figure 2 shows a closing of energetically forbidden Coster-Kronig channels for Fe ion ground states at increasing ion charge state q. The results have been obtained from DFS calculations. The transitions energies are approximately computed using the (Z+1) rule

$$E(n_1l_1 \rightarrow n_2l_2n_3l_3) = E_{Bn_1l_1}(Z) - \frac{1}{2}[E_{Bn_2l_2}(Z) + E_{Bn_2l_2}(Z+1) + E_{Bn_3l_3}(Z) + E_{Bn_3l_3}(Z+1)],$$

where E_B(Z) and E_B(Z+1) are the binding energies for the shells n_1l_1, n_2l_2 and n_3l_3 in atoms with Z and Z+1 atomic numbers, respectively. The non-radiative transition allowed under this condition is

$$E_{Bn_1l_1}(Z)\rangle\frac{1}{2}[E_{Bn_2l_2}(Z) + E_{Bn_2l_2}(Z+1) + E_{Bn_3l_3}(Z) + E_{Bn_3l_3}(Z+1)].$$

Figures 3 and 4 show ion charge state distributions (CSD), q, produced after creation of the primary K-, L_I- and L_{III} vacancies in neon and argon atoms, in comparison with other theoretical values from Opendak [18] and experimental results [3]. It is found from the comparison that the selection of atomic data and the consideration of secondary effects during vacancy cascade development improve the agreement

between the calculated values and the experimental spectra. We see that neon has two-fold ionization, as demonstrated by the ion charge state following de-excitation of the K-shell primary vacancy. That is because after K-shell ionization in neon, the probability of Auger K-LL is higher than the K-fluorescence yield. As a result of Auger transition K-LL, two-fold ionization (Ne^{2+}) is dominant. The resulting ionization are higher than two-fold due to shake-off processes in elements up to neon. Ar^{4+} is dominant in Argon because more KLM and LLM non-radiative transitions contribute to the vacancy cascades. The average number of additional ejected electrons as a function of the primary ionization state of ions can be obtained from the sum $\bar{q} = \sum qp(q)$, where q is the degree of ionization and $p(q)$ is the propability of ejected electrons. The results obtained for the average charge state ionization as function of initial inner shell vacancy agree well with the corresponding experimental data.

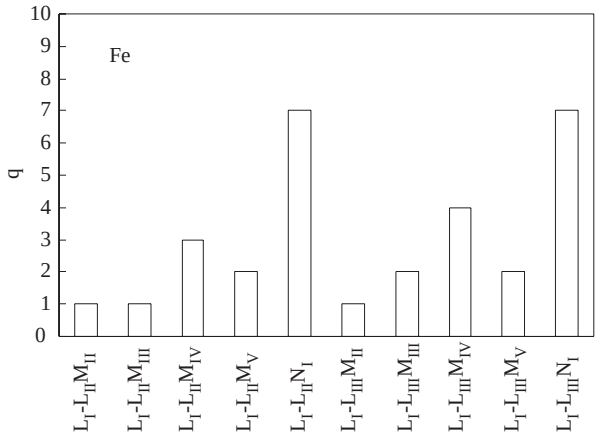

Figure 2. Closing of energy forbidden Coster-Kronig transitions for iron ground states with increasing ion charge state q.

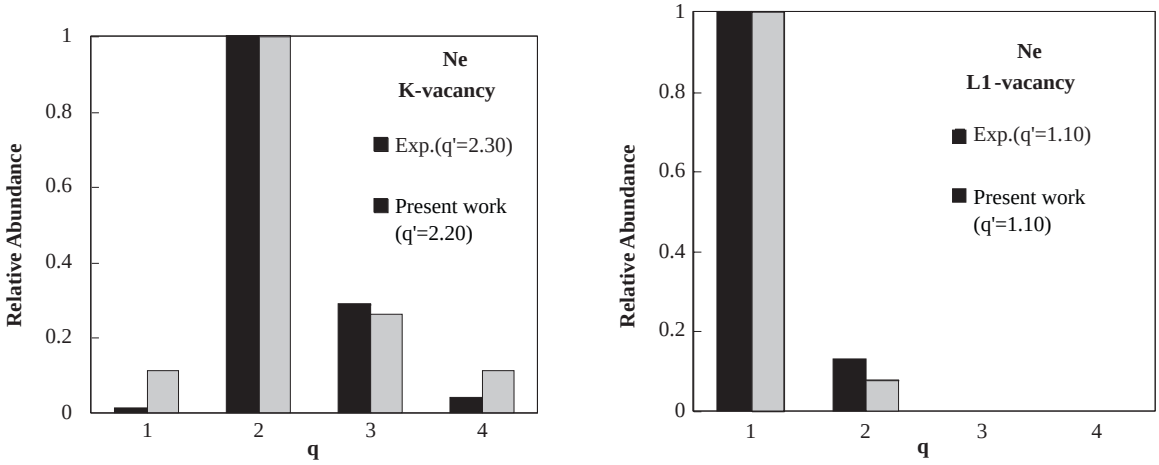

Figure 3. Ion charge distribution (CSD) q produced after K-, and L_I shell in neon.

Figure 5 shows the ion charge state distributions (CSD) following after K-, L_I- and L_{III}- vacancies in Fe atom (Z=26). The ion charge states are shown as complex spectrum in Fe atom, because the atomic structure in Fe is complex in comparison with the atomic structure of argon and neon atoms. The increasing number of Auger and Coster-Kronig transitions is due to a higher ion charge distributions (CSD).

Tables (1-4) show the dependence of average ion charge states $\bar{q}$ on the degree of ionization (i = 1 to 10) after de-excitation of K-, L_I-, L_{III}- , and M_I sub-shells vacancies in elements with atomic number Z from 6 to 26. The tabulated results show that the deeper vacancies lead to higher average ion charge states ($\bar{q}$). But, the primary vacancies in outer-shells produce ions charge states with small ionization degree, because during vacancy cascade development the number of possible de-excitation channels is restricted. The tabulated results indicate that the average ion charge states q increase with increasing atomic number Z.

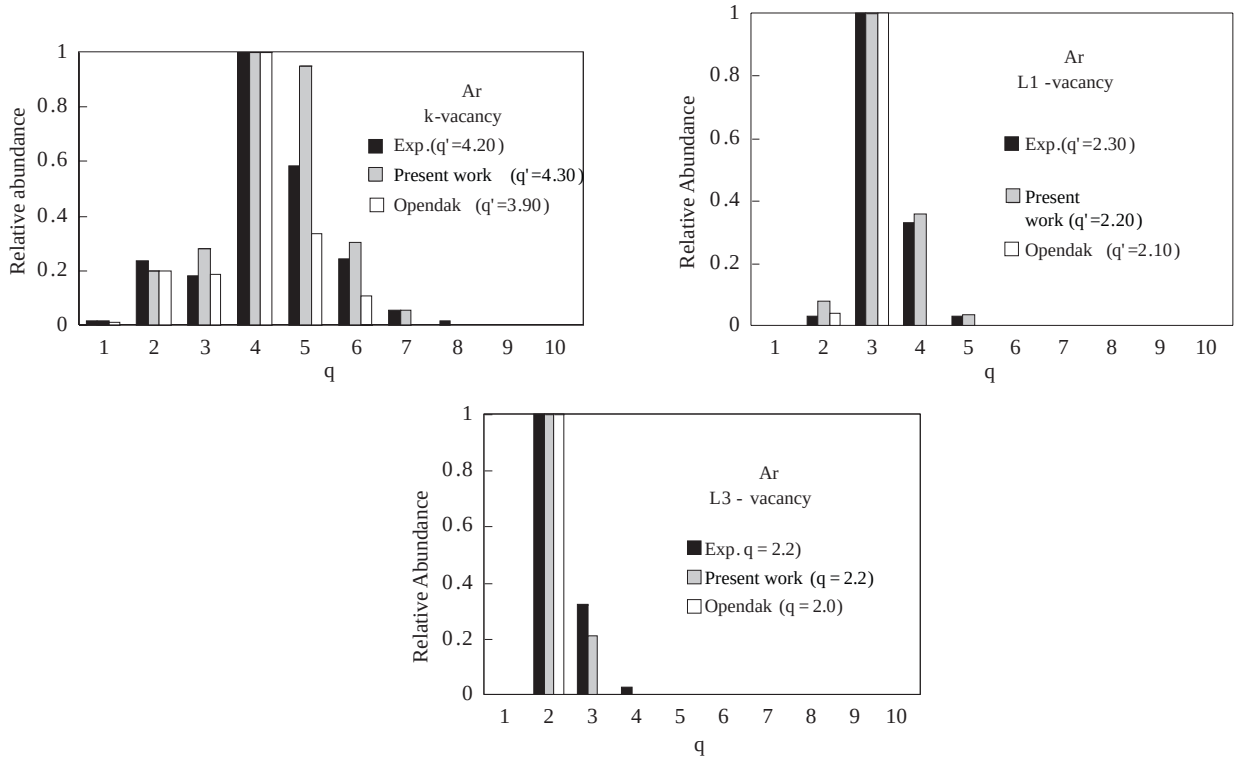

Figure 4. Ion charge distribution (CSD) q produced after K-, L_I, and L_{III} shell in argon.

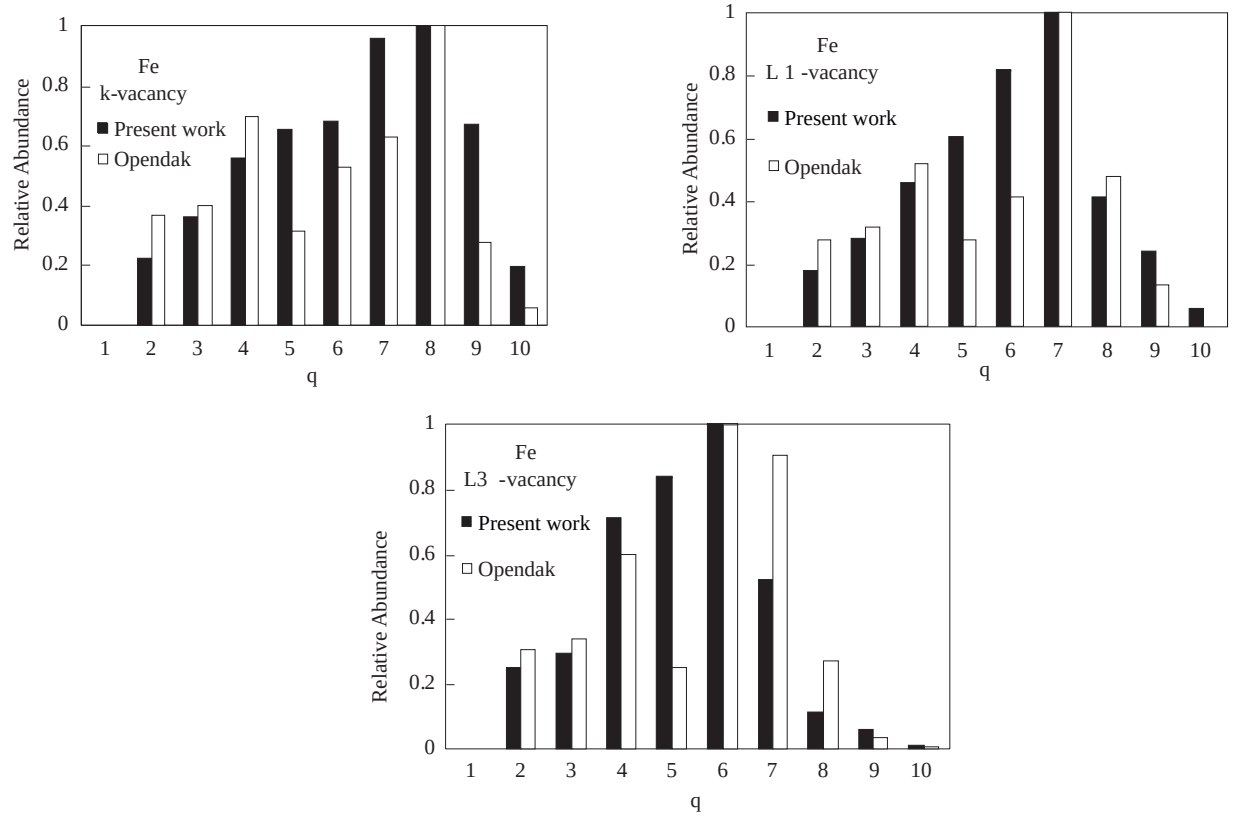

Figure 5. Ion charge distribution (CSD) q produced after K-, L_I and L_{III} shell in iron.

Table 1. The average ion charge states following K-shell ionization for neutral atoms and ground state ions from Z = 6 to Z = 26.

Z \ q	0	1	2	3	4	5	6	7	8	9	10
6	1.99	1.99	1.99	1.00							
7	1.01	1.00	1.00	1.00							
8	1.97	1.98	1.00	1.00							
9	1.96	1.97	1.97	1.00							
10	2.22	2.21	2.19	2.18	2.07	2.06	2.01	1.02	1.00	1.00	1.00
11	2.34	1.98	1.98	1.98	1.98	1.97	1.96	1.99	1.00	1.00	1.00
12	3.44	2.71	2.09	2.09	2.08	2.07	2.00	1.99	1.00	1.00	1.00
13	3.98	3.25	2.74	2.11	2.01	2.08	2.00	1.99	1.00	1.00	1.00
14	4.51	3.86	3.16	2.27	2.02	2.01	2.01	1.99	1.94	1.93	1.00
15	4.12	3.91	3.24	2.99	2.52	1.94	1.94	1.93	1.92	1.89	2.00
16	4.11	4.05	3.86	3.21	2.89	2.24	1.92	1.92	1.92	1.89	1.87
17	4.04	4.04	3.20	3.79	3.19	2.88	1.92	1.97	1.92	1.90	1.89
18	4.37	4.34	4.30	4.16	3.81	3.30	2.90	2.81	1.90	1.85	1.90
19	4.32	3.83	3.83	3.83	3.82	3.64	3.09	2.93	1.86	1.87	1.85
20	5.13	3.74	3.62	3.80	3.79	3.73	3.60	3.56	2.81	2.74	1.84
21	3.74	3.75	3.75	3.45	3.75	3.74	3.68	3.60	3.45	2.82	1.80
22	5.66	5.07	4.42	4.05	3.95	3.80	3.70	3.65	3.60	2.99	2.73
23	6.12	5.20	4.63	4.37	4.13	3.91	3.79	3.68	3.68	3.08	3.01
24	6.20	5.34	4.67	4.11	4.09	3.93	3.74	3.52	3.50	3.41	3.18
25	6.38	5.66	4.72	4.10	4.07	3.99	3.75	3.53	3.52	3.50	3.44
26	6.39	5.93	5.16	4.58	4.29	4.08	5.09	3.64	3.43	3.44	3.42

Table 2. The average ion charge states following L_I-shell ionization for neutral atoms and ground state ions from Z = 6 to Z = 26.

Z \ q	0	1	2	3	4	5	6	7	8	9	10
6	1.00	1.00	1.00								
7	1.00	1.00	1.00								
8	1.00	1.00	1.00								
9	1.00	1.00	1.00								
10	1.08	1.07	1.07	1.06	1.02	1.01	1.00	1.00	1.00	1.00	1.00
11	1.99	1.00	1.00	1.00	1.00	1.00	1.00	1.00	1.00	1.00	1.00
12	2.27	2.19	1.03	1.03	1.03	1.02	1.00	1.00	1.00	1.00	1.00
13	2.48	2.25	1.14	1.03	1.03	1.02	1.00	1.00	1.00	1.00	1.00
14	3.6	3.44	2.19	2.08	1.03	1.02	1.01	1.01	1.00	1.00	1.00
15	2.98	2.98	2.98	2.00	2.00	1.00	1.00	1.00	1.00	1.00	1.00
16	2.97	2.97	2.97	2.98	2.00	2.00	2.00	1.00	1.00	1.00	1.00
17	2.97	2.97	2.97	2.97	2.97	2.00	2.00	1.00	1.00	1.00	1.00
18	3.24	3.23	3.20	3.13	3.03	2.96	2.02	1.02	1.00	1.00	1.00
19	3.55	2.96	2.96	2.96	2.96	2.96	2.95	2.00	2.00	1.00	1.00
20	4.13	3.83	3.04	3.04	3.02	3.00	2.95	2.92	2.00	1.00	1.00
21	2.95	2.95	2.95	2.95	2.95	2.95	2.94	2.93	2.94	2.00	1.99
22	4.76	4.15	3.13	3.11	3.10	3.06	2.95	2.93	2.89	2.84	2.00
23	5.26	4.32	4.19	3.15	3.11	3.09	2.96	2.94	2.88	2.85	2.08
24	5.48	4.61	4.22	3.18	3.21	3.19	2.99	2.94	2.89	2.99	2.57
25	5.51	4.92	4.00	3.27	3.25	3.21	3.13	2.95	2.95	2.94	2.91
26	5.57	5.29	4.68	4.17	4.01	3.88	3.42	3.10	2.95	2.94	2.94

Table 3. The average ion charge states following L_{III}-subshell ionization for neutral atoms and ground state ions from Z = 6 to Z = 26.

Z \ q	0	1	2	3	4	5	6	7	8	9	10
6											
7											
8											
9											
10	1.03	1.02	1.01	1.00	1.00	1.00	1.00	1.00	1.00	1.00	1.00
11	1.00	1.00	1.00	1.00	1.00	1.00	1.00	1.00	1.00	1.00	1.00
12	2.18	1.19	1.01	1.01	1.00	1.00	1.00	1.00	1.00	1.00	1.00
13	2.72	1.74	1.88	1.05	1.00	1.00	1.00	1.00	1.00	1.00	1.00
14	2.99	2.94	2.35	1.35	1.01	1.00	1.00	1.00	1.00	1.00	1.00
15	1.99	1.99	1.99	1.99	1.00	1.00	1.00	1.00	1.00	1.00	1.00
16	1.99	1.99	1.99	1.99	1.99	1.00	1.00	1.00	1.00	1.00	1.00
17	1.99	1.99	1.99	1.99	1.99	1.00	1.00	1.02	1.00	1.00	1.00
18	2.18	2.18	2.08	2.16	2.08	2.06	2.00	1.98	1.00	1.00	1.00
19	2.23	1.99	1.99	1.99	1.99	1.98	1.99	2.02	1.00	1.00	1.00
20	3.23	2.46	2.10	2.08	2.08	2.08	2.02	198	1.98	1.97	1.00
21	1.99	1.99	1.99	1.99	1.99	1.99	1.99	2.09	1.98	2.00	1.00
22	3.95	3.09	2.89	2.88	2.82	2.35	2.09	2.10	2.00	2.00	1.97
23	3.98	3.74	3.05	2.90	2.81	2.51	2.12	2.03	2.00	2.00	2.00
24	4.01	3.81	3.13	2.99	2.87	2.67	2.13	2.02	2.00	2.02	2.00
25	4.19	3.89	3.26	3.03	3.02	2.81	2.15	2.13	2.03	2.02	2.02
26	4.10	3.99	3.61	3.55	3.76	3.09	2.81	3.13	2.02	2.02	2.02

Table 4. The average ion charge states following M_I-subshell ionization for neutral atoms and ground state ions from Z = 6 to Z = 26.

Z \ q	0	1	2	3	4	5	6	7	8	9	10
6											
7											
8											
9											
10											
11											
12	1.00										
13	1.00										
14	1.00										
15	1.00										
16	1.00										
17	1.00										
18	1.00	1.00									
19	1.99	1.00									
20	2.25	1.98									
21	2.44	2.15									
22	2.97	2.94	2.01								
23	3.10	3.09	2.91								
24	3.22	3.10	3.01	2.55							
25	3.24	3.15	3.08	3.03	3.02	2.06	2.04				
26	2.25	3.18	3.10	3.09	3.06	3.02	2.05	2.04			

4. Conclusion

- Ion charge state distributions (CSD) and mean charged ions produced after inner ionization in neutral atoms and ion ground state ions for elements from Z = 6 to Z = 26 have been calculated.
- Atomic data for radiative transition rates and electron shake-off have been calculated using MCDF wavefunctions, and non-radiative transition rates have been obtained by DFS wavefunctions.
- The selection of atomic data is important to accurately model the vacancy cascades.
- Considering the electron shake off probabilities and closing of some Coster Kronig channels, which are energetically forbidden during vacancy cascades propagation, enhance the agreement between present calculation and the experimental data.

Acknowledgement

We would like to thank Ali H. Abdullah for his important contributions to this work.

References

[1] A.H. Snell In Alpha-, Beta- and Gamma- Spectroscopy (Edited by Siegbahn K.), p. 1545 North- Holland, Amsterdam.

[2] T. A. Carlson and M.O. Krause, *Phys. Rev.,* **137A,** (1965), 1655.

[3] T.A. Carlson, W. E. Hunt and M.O. Krause, *Phys. Rev.,* **151,** (1966), 41.

[4] M.O. Krause and T.A. Carlson, *Phys. Rev.,* **158,** (1967), 18.

[5] T.B. Hastings and V.O. Kostroum, *Nucl. Instr. Methods,* **208,** (1983).

[6] T. Tonuma, A. Yagishita, H. Shibata, T. Koizumi, T. Matsua, K. Shima, T. Mukoyama and H. Tawara, *J. Phys.* **B20**, (1987), L31.

[7] T. Hayaishi, Y. Morioka, Y. Kageyama, M. Watanabe, I. H. Suzuki, A. Mikuni, G. Isoyama, S. Asaoka and M. Nakamura, *J. Phys. B: At. Mol. Phys.,* **20,** (1987), L287.

[8] T. Mukoyama, T. Tonuma, A. Yagishita, H. Shibata, T. Koizumi, T. Matsuo, K. Shima and H. Tawara, *J. Phys. B: At. Mol. Phys.,* **20,** (1987), 4453.

[9] T. Mukoyama and K. Shima, *Bull. Inst. Res., Kyoto Univ.,* **69**, (1991), 29.

[10] J.C. Weisheit, *Astrophys. J.,* **190,** (1974), 735.

[11] R.T. Short, D.A. Church, S.D. Kravis, I.A. Sellin, J.C. Levin, M. Meron, B.M. Johnson and K.W. Jones, *Phys. Rev.,* **A36,** (1987), 2484.

[12] G.D. Shirkov and G. Zschornack, (1996) Electron Impact Ion Sources for Highly Charged Ions. Vieweg-Verlag, Wiesbaden.

[13] Ch. Heinzelmann, U. Lehnert, D. Kuchler and G. Zschornack, *Hyperfine Interactions,* **108,** (1997), 51.

[14] G. Omar and T. Hahn, *Phys. Rev.,* **A43,** (1991), 9.

[15] T.A. Carlson and M.O. Krause, *Phys. Rev.,* **A140,** (1965), 1057.

[16] T. Mukoyama, *J. Phys. Soc. of Japan,* **55,** (1986), 3054.

[17] M.N. Mirakhmedov and E.S. Parilis, *J. Phys.,* **B21,** (1988), 795.

[18] M.G. Opendak, *Astrophysics and Space Science,* **165,** (1990), 9.

[19] J.H. Scofield, *Atom. Data Nucl. Data Tables,* **14,** (1974), 121.

[20] E.J. McGuire, *Phys. Rev.,* **A2**, (1970), 273.

[21] M.H. Chen and B. Crasemann, *Phys. Rev.,* **A35,** (1987), 4579.

[22] D.L. Walters and C.P. Bhalla, *Atom. Data,* **3,** (1971), 301.

[23] I. Reiche, (1992), Doctoral Thesis TU Dresden, Fakultat fur Mathematik und Naturwissenschaften, Dresden.

[24] I.P. Grant, B.J. McKenzie, P.H. Norrington, D.F. Mayers and N.C. Pyper, *Comp. Phys. Comm.,* **21,** (1980), 207.

[25] I.P. Grant and B.J. McKenzie, *J. Phys.,* **B13,** (1980), 2671.

[26] B.J. McKenzie, I.P. Grant and P.H. Norrington, *Comp. Phys. Comm.,* **21,** (1980).

[27] M. Lorenz and E. Hartmann, ZfI- 109, Leipzig p27, (1985).

[28] A. El- Shemi, *Egypt. J. Phys.,* **27**, No. 1-2 pp. (1996) 231.

[29] A.M.M. Mohammedein, I. Reiche and G. Zschornack, *Rad. Effects and Defects in Solids,* **129,** (1993), 309.

[30] A.M.M. Mohammedein, G. Zschornack, *Wissenschaftliche Zeitschrift der TU Dresden,* **43,** (1994), Heft 2, 26.

[31] Adel M. El-shemi, Adel A. Ghoneim, Ali H. Abdullah, Association for the advancement of modelling & simulation techniques in enterprises (A.M.S.E) V. 73 , N 3,4 (2000), 41-58.

[32] F.P. Larkins, *J. Phys. B: At. Mol. Phys.,* **4,** (1971), L29.